Design and Analysis of a Low Voltage Simulink Model (LVSM) of IEEE 57 Bus

G. VEERA BHADRA CHARY, RAGHAVAIAH KATURI*, K. MERCY ROSALINA
Department of Electrical and Electronics Engineering,
Vignan's Foundation for Science Technology and Research deemed to be a University,
Guntur, Andhra Pradesh,
INDIA

*Corresponding Author

Abstract: - The present power system is gaining momentum towards designing equivalent circuit models. The Ward and REI methods involve the admittance reduction method as well as being merged with the EMS model to derive boundary parameters, but these methods are limited and valid for a predefined condition. Therefore, it is required to design an equivalent circuit that adopts the real power system for analysis. In this paper, a new method is proposed to design a scaled-down power system model without changing the impedance of components. In this regard, a Low Voltage Simulink Model (LVSM) of the IEEE 57 bus network was designed in MATLAB/ Simulink so that it could be useful for laboratory model design purposes. The main objectives of this paper are to propose a mathematical procedure to scale down the network parameters and design a 3-phase LVSM of an IEEE 57 bus power system network within the Simulink platform. The performance of LVSM was analyzed with no-load, balanced load, and unbalanced load models. These simulation studies were validated and compared with the theoretical results to prove that the proposed LVSM modeling has good mathematical accuracy, robustness, and validity for practical model implementation.

Key-Words: - Boundary parameters, equivalent circuit, IEEE 57 bus, LVSM, MATLAB / Simulink, real power system, scale-down power system model.

Received: February 23, 2023. Revised: December 7, 2023. Accepted: December 19, 2023. Published: March 12, 2024.

Nomenclature

i ith Bus / Load / Generator component
$|V|_{tmi}, |I|_{tmi}$ Voltage and Current in test case system
$|P|_{tmi}, |Q|_{tmi}$ Active and Reactive powers in test case system
$|V|_{sdi}, |I|_{sdi}$ Voltage and Current in LVSM
$|P|_{sdi}, |Q|_{sdi}$ Active and Reactive Powers in LVSM
R_{tmi}, X_{tmi} Resistance and Reactance in test case system
R_{sdi}, X_{sdi} Resistance and Reactance in LVSM
$|\delta|_{tmi}, |\emptyset|_{tmi}$ Voltage and Current angle in test case system
$|\delta|_{sdi}, |\emptyset|_{sdi}$ Voltage and current angle in the LVSM

1 Introduction

The power system engineers always strive to design practical models of big power system networks to predict practical outcomes. In earlier days, there were Analog equivalent models; in these transmission lines, basic elements and generators represented variable voltage sources. After that, digital simulation was born. In this, the digital computer is used for load flow and other problems. Nowadays, the complexity of the power system has increased drastically due to the addition of renewable sources, power converters, and smart technologies, [1]. At present, real-time simulation (RTS) is used for modeling; this modeling is categorized as long-term modeling for planning purposes, short-term modeling, and -time modeling for operational management. Table 1 shows various software packages used for the type of modeling, purpose, and study. Apart from those, there are commercial software programs that model the power system in economic and market aspects, [2]. Various types of digital real-time simulators (DRTS) for modeling, hardware, software, communication interfacing, I/O protocols, solution methods, and applications are explained in detail, [3].

MATPOWER has facilitated an extensive suite of tests to ensure quality code. Many researchers are using MATLAB to find the testing framework for designing their own MATLAB programs. There are various software packages used for power system simulation developed by the researchers. MATLAB and Simulink have been supported in designing the power system, which includes power electronics, FACTS, control systems, renewable sources, etc. The state-space modeling and GUI-based PSB components are discussed in, [4]. Simulink has been developed as an educational package since 1997. ULg collaborated with Bologna University and developed various traditional components such as synchronous generators, transmission lines, transformers, etc. in the Electrical Energy Systems Lab of NTUA, [5]. A Power Analysis Toolbox (PAT) was developed by West Virginia University's Advanced Power Engineering Research Centre (APERC). It includes facts and is flexible enough to perform load flow, transient, and small signal analysis of power systems, [6], [7]. Mat Dyn is open-source software meant to focus on transient stability analysis and time domain simulation. The design criteria, advantages, and code structure are discussed in, [8], [9]. The PSAT was the first open-source software that ran on the GNU/Octave and network editor to perform power system analysis. Other than those features, it has continuation power flow (CPF), GUI, and GNE, [10]. It has been used by many universities for teaching both UG and PG courses and has also formed an online virtual laboratory to support students via the Internet, [11], [12].

The "PowSim" simulator was designed by the University of Bath for real-time simulations; the operation of the algorithm was verified on IEEE 57 bus traditional methods and the reduced British National grid system, [13], together with knowledge-based systems, [14]. Dynamic modeling and analysis with real-time simulators; Hydro-QuObec (IREQ) in, [15], reduction of a power system to a dynamic equivalent model in, [16], as well as generator dynamics and transient disturbances in, [17]. For information analysis of future power systems, an architecture was proposed; it has an alternate communication network that adopts suitable computing, [18]. Interfacing the simulator with the physical power system is an improvement in hardware testing by using Kron's method of network tearing, components, and procedure, discussed in, [19]. Several ways of probabilistic-based modeling and diagnosis by using Bayesian networks (BN) and arithmetic circuits (ACs) are discussed in, [20]. The Energy Management System (EMS) has a limited part of the interconnected system; therefore, an equivalent circuit is required to determine operating constraints offline. Other than the Ward and REI methods, based on boundary-measured parameters (voltage, angle, and powers), an equivalent circuit is designed in, [21].

Table 1. Simulation software's for power system analysis and modeling

S.no.	Modeling / Analysis	Type of Study	Software Package
1	Dynamic	dynamic voltage control, Transient stability, critical clearing time, faults	DINIS, DIgSILENT, ERACS, ETAP, IPSA, PSS/E, SKM Power Tools, Power World,
2	Steady State	Load flow, DG's contribution, Fault level, Voltage step	DIgSILENT, DINIS, ERACS, IPSA, Open DSS, ETAP, Power World, PSS/E, SKM Power Tools,
3	Electro Magnetic Transient (EMT)	FACTS / HVDC design, SSR, Insulation coordination	ATP-EMTP, EMTP-RV, PSCAD/ EMTDC
4	Real-Time Simulation (RTS)	Protection and Control testing; Real-time simulations	Opal-RT, RTDS
5	Multi-Domain Analysis	Electrical, Power Electronics, Mechanical, and Fluid dynamic systems.	MATLAB (including Simulink and SPS/Simulink), DYMOLA
6	Hybrid Simulation	Dynamic analysis between two systems	ETRAN (PSS/E and PSCAD)
7	Harmonic Analysis	Impedance scan, Load flow with VSC	DIgSILENT, ERACS, ETAP, IPSA, PSS Sincal, SKM Power Tools

Without admittance reduction, with boundary-measured parameters, a new methodology is proposed in this paper, which mainly focuses on scale-down bus-measured parameters by keeping impedance constant for all components such as transmission lines, synchronous generators, transformers, loads, etc. Therefore, the size and operating ranges (voltage, current, and power) of every component are scaled, making it easy to design a power system. This paper designs a 3-phase low-voltage Simulink Model (LVSM) of the IEEE 57 bus test case system in Simulink. The test case data and power system one-line diagram obtained from, [22], scale down according to the methodology. The performance of LVSM was obtained from the no-load, balanced load, and unbalanced load simulations. Thus, simulation results show power flows in lines and bus powers, as well as voltage, angle, and currents. These analyses prove the accuracy of the methodology and LVSM validity while designing the model.

The other sections are organized as follows: Section II discusses the proposed methodology and LVSM design. Section III explains the simulation results of three load tests. The key points of the results and the scope of future work are discussed in Section V.

2 Methodology and LVSM Design

The Scale-Down modeling concept in this paper discusses two main steps, first, scale the ratings of all components according to the proposed method, and second, develop a 3-phase equivalent power system model in MATLAB / Simulink.

2.1 Proposed Mathematical Procedure

In order to develop LVSM, consider standard power system data of all components such as voltage, current, powers and line parameters. The present concept relies on the following assumptions.

- Balanced power system network.
- Magnitude of phase angle independent of scaled voltage.
- The magnitude of resistance, reactance, and shunt component remain the same irrespective of its current.
- Therefore, p.f will be the same in both cases.
- All transmission lines are assumed to be as per km distributed pi model lines (R=0).
- Temperature assumed to be constant.
- With the above assumptions, the following conditions are also used to derive the methodology.
- The voltage of any component directly proportional to the current (V $\alpha\, I$).
- Active and Reactive power of load/generator / bus directly proportional to the square of its voltage (P $\alpha\, V^2$ and Q $\alpha\, V^2$) .

Let us consider a power system network, to Scale down each component rating consider the standard data such as voltage, current, and powers w.r.t its bus. Define the operating voltage of the model according to the design requirement and find the scaling factor of voltage, which is known as the Voltage Scaling Factor (VSF). It can be defined as "the ratio magnitude of test case voltage ($|V|_{tmi}$) to scale down voltage ($|V|_{sdi}$) ith component of in the network by assuming magnitude of phase angles equal ($|\delta|_{tmi} = |\delta|_{sdi}$)".

$$\mathrm{V.S.F} = \frac{|V|_{\mathrm{tmi}}}{|V|_{\mathrm{sdi}}} \tag{1}$$

Similarly, Current Scaling Factor (CSF) is also used to scale down the current rating of the component in the network. It can define as "the ratio of the current (I_{tmi}) of component in the test case to scale down current (I_{sdi}) of ith component in the network by assuming magnitudes of phase angles equal ($|\emptyset|_{tmi} = |\emptyset|_{sdi}$)".

$$C.S.F = \frac{|I|_{tmi}}{|I|_{sdi}} \tag{2}$$

Consider active and reactive powers of load / generator / transformer, either (1) or (2) equation is using for calculation of new power rating of the component.

Active power ($|P|_{tmi}$) of actual network defined as:

$$|P|_{tmi} = \frac{|V|^2_{tmi}}{R_{tmi}} \tag{3}$$

Similarly, for LVSM $|P|_{sdi}$ as,

$$|P|_{sdi} = \frac{|V|^2_{sdi}}{R_{sdi}} \tag{4}$$

$$\forall \quad R_{sdi} = R_{tmi} \tag{5}$$

∴ From equations (3), (4) and (5),

$$\frac{|P|_{tmi}}{|P|_{sdi}} = \frac{|V|^2_{tmi}}{|V|^2_{sdi}} \tag{6}$$

However,

$$\frac{|P|_{sdi}}{|P|_{tmi}} = \frac{1}{V.S.F^2} \tag{7}$$

$$\therefore \ \forall \ |P|_{sdi} = \frac{|P|_{tmi}}{V.S.F^2} \tag{8}$$

Reactive power ($|Q|_{tmi}$) of actual network defined as:

$$|Q|_{tmi} = \frac{|Q|^2_{tmi}}{X_{tmi}} \tag{9}$$

Similarly, for LVSM $|Q|_{sdi}$ as,

$$|Q|_{sdi} = \frac{V^2_{sdi}}{X_{sdi}} \tag{10}$$

$$\forall \quad X_{sdi} = X_{tmi} \tag{11}$$

From equations (9), (10) and (11),

$$\frac{|Q|_{tmi}}{|Q|_{sdi}} = \frac{|V|^2_{tmi}}{|V|^2_{sdi}} \tag{12}$$

However,

$$\frac{|Q|_{sdi}}{|Q|_{tmi}} = \frac{1}{V.S.F^2} \tag{13}$$

$$\therefore \forall |Q|_{sdi} = \frac{|Q|_{sdi}}{V.S.F^2} \tag{14}$$

The equations (1), (2), (8) and (14) are used to calculate the voltage and power ratings of LVSM components. However, CSF can also use to calculate power ratings as well as losses of the equipment.

2.2 IEEE 57 Bus Test Case LVSM

The methodology proposed in the previous section is used to design the IEEE 57 bus test case as LVSM, it consists of 7 voltage sources, 57 buses, 9 distribution transformers, 6 voltage regulating transformers, and 63 pi-model transmission lines. The structure of 3- phase LVSM designed in MATLAB / Simulink as per scaled bus voltage and powers of load / generator / transformer as shown in Figure 1. Whereas the total network identified as two sub-networks SN1 and SN2; red highlighted SN1 (1 - 17 buses) has 414 (l-l) volts as well as SN2 (18 - 57 buses) has 207 (l-l) volts.

The standard data of the test case system corresponds to the balanced network; therefore, the calculated parameters of all components also correspond to the balanced LVSM. The transmission lines are composed of per km distributed pi sections, each section parameters are Rs=0.12 Ω / km, Ls=1.5273 mH / km and Csh=0.02 MFD/km (typical line parameters of 138kv line) without mutual coupling between lines, [23]. As per the line parameters data, for each line no. of pi section and length calculated. All generators are voltage sources which supply balanced voltage, and every load is termed as constant PQ balanced load. Each bus is considered as a boundary point to connected lines, which is used to measure voltage, angle, and power injection to the connected lines.

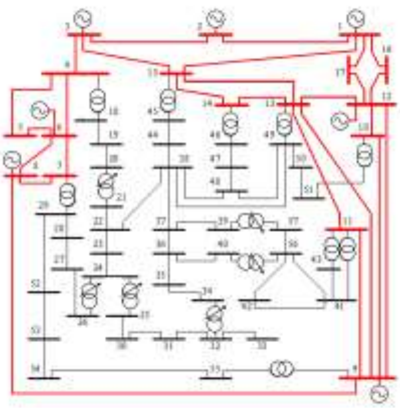

Fig. 1: 3-phase equivalent one-line diagram of IEEE 57 bus test case network

3 Results Analysis

The steady-state simulation carried out with the discretized 3-phase LVSM Simulink model, with a time step of $50\mu s$ and simulation performed for 1s. Three simulation studies were considered to assess the accuracy and robustness of LVSM while designing a practical model. Those are the No-load test which does not consider the load at buses, the Balanced-load which consists of balanced distribution of load at buses and the Unbalanced-load which considers the unbalanced distribution of load at buses. All these simulations verify the boundary (bus) parameters such as voltage, angle, and powers at buses as well as power flow through the π-model lines and distribution / voltage regulating transformers. In each test case, the simulation results analyzed sub-network as shown in Figure 1.

3.1 No-load LVSM

In this test, the voltage shown at the bus has an error due to the small current through lines, Table 2 and Table 3 show results corresponding to the 'R' phase only. It can be observed that bus 14 draws more reactive power so that it has a 2.86% voltage error, as well as due to more active power at bus 9 cause the largest current of 0.37amp in SN1.

Table 2. Phase R: No-load simulation results of 414(l-L) voltage buses

Bus no.	V_R volts (rms)	Angle (deg.)	I_R amps (rms)	Angle (deg.)	P_{RYB} watts	Q_{RYB} var
1	238.62	-0.21	0.17	-16.76	115.8	34.17
2	238.79	-0.14	0.11	-14.00	76.37	18.66
3	238.18	-0.29	0.26	-26.57	165.7	81.46
4	238.56	-0.32	0.05	89.80	0.124	-34.76
5	239.09	-0.24	0.02	-171.43	-12.16	1.87
6	238.99	-0.18	0.13	5.89	95.09	-9.996
7	237.62	-0.51	0.11	-38.33	59.53	46.25
8	238.57	-0.24	0.19	-16.71	129.2	38.01
9	237.76	-0.41	0.37	-28.32	234.1	123.4
10	237.96	-0.72	0.05	-1.32	35.65	0.537
11	235.34	-1.00	0.15	101.98	-24.06	-100.8
12	237.83	-0.40	0.36	-27.52	228.3	116.11
13	233.07	-0.98	0.12	137.63	64.64	-56.98
14	232.16	-1.12	0.32	-57.45	123	182.8
15	235.27	-0.84	0.36	-39.71	197.5	158.7
16	238.53	-0.38	0.03	-59.40	12.32	20.49
17	238.87	-0.32	0.02	1.05	12.5	-0.317

As shown in Table 3, in SN2 almost all the buses show negative voltage error because of the absence of loads, but bus 26 show 1.15% error. It was observed bus 49 drew more active and reactive powers as well as current; therefore, it has more voltage than all other buses.

Table 3. Phase R: No-load simulation results of 207(L-L) voltage buses

Bus no.	V_R volts (rms)	Angle (deg.)	I_R amps (rms)	Angle (deg.)	P_{RYB} watts	Q_{RYB} var
18	122.84	-0.43	0.07	-23.70	23.97	10.29
19	120.99	-1.28	0.08	-40.27	23.75	19.23
20	119.39	-1.77	0.10	-47.92	23.58	24.59
21	124.53	-1.77	0.16	133.90	-41.62	-40.52
22	125.28	-1.55	0.15	135.12	-41.73	-39.22
23	125.17	-1.59	0.18	-44.09	51.05	46.64
24	123.19	-2.17	0.19	-46.29	50.69	49.04
25	123.17	-2.18	0.03	74.15	2.723	-10.84
26	118.13	-2.16	0.29	-42.53	79.66	67.57
27	121.07	-1.14	0.29	-41.10	80.47	67.27
28	122.16	-0.77	0.29	-40.55	80.77	67.09
29	122.82	-0.54	0.20	-21.81	69.39	27.12
30	123.40	-2.24	0.02	69.54	2.695	-7.996
31	123.64	-2.36	0.01	17.21	2.636	-0.925
32	123.15	-2.42	0.03	-77.41	2.546	9.798
33	123.15	-2.42	0.00	0.00	0	0
34	120.08	-2.42	0.21	-43.36	58.1	50.23
35	120.75	-2.19	0.21	-42.76	58.23	49.68
36	121.20	-2.04	0.21	137.65	-58.32	-49.29
37	122.23	-1.95	0.74	-59.82	144.6	227.8
38	125.69	-1.43	0.31	75.94	24.46	-112.9
39	122.00	-2.05	0.17	-34.13	53.43	33.6
40	120.26	-2.03	0.41	-79.88	32.08	143.5
41	123.24	-1.02	0.10	-118.09	-16.89	33.36
42	124.46	-1.54	0.09	-121.99	-16.73	28.77
43	122.90	-1.00	0.02	94.51	-0.8944	-8.995
44	124.89	-1.25	0.31	76.03	24.67	-113
45	123.19	-0.85	0.32	76.23	25.13	-113
46	128.92	-1.14	0.33	-66.01	55.39	116
47	127.83	-1.23	0.33	-66.21	55.1	116
48	127.45	-1.27	0.34	-66.28	55	116
49	130.07	-1.01	1.04	-67.86	162.2	372.8
50	129.31	-0.91	0.13	-93.30	-1.587	49.11
51	127.95	-0.73	0.14	-93.14	1.755	51.98
52	123.82	-0.52	0.11	106.42	-11.66	-37.49
53	124.33	-0.51	0.10	107.05	-11.71	-36.23
54	125.44	-0.47	0.09	108.71	-11.82	-33.16
55	126.43	-0.43	0.09	110.67	-11.91	-30.06
56	125.46	-2.03	0.07	107.61	-9.239	-25.31
57	124.49	-2.06	0.08	105.21	-9.154	-28.89

3.2 Balanced Loads LVSM

With the addition of constant PQ load at buses, the LVSM equivalent to the scale-down model of the IEEE 57 bus test case system. Since all loads equally distributed among R Y B phases; therefore, results have shown w.r.t ‘R’ phase, and the Table 4 and Table 5 results considered only load buses. Bus 14 is connected to the transformer, which is more loaded than the 12th bus; therefore, it has 8.37% more error in SN1. However, the current drawn by this bus is 4.83amp, which is more than the remaining buses because of a large connected load.

Table 4. Phase R.: Balanced loads simulation results of 414(L-L) voltage buses

Bus no.	V_R volts (rms)	Angle (deg.)	I_R amps (rms)	Angle (deg.)	P_{RYB} watts	Q_{RYB} var
1	233.16	-2.24	1.90	-25.36	1219	519
2	233.22	-1.24	1.34	-41.18	718.1	600
3	232.83	-2.31	1.97	-26.05	1258	551
5	233.84	-2.87	0.04	114.07	-14.09	-27.4
6	235.36	-2.39	1.83	-13.37	1267	244.7
8	233.33	-3.28	2.54	-16.35	1729	400.3
9	230.70	-4.01	3.19	-20.73	2110	632.2
10	225.73	-6.84	0.15	-50.48	71.15	68.09
12	228.37	-6.32	4.83	-17.45	3242	635.7
13	220.31	-6.80	0.15	92.82	-16.59	-97.57
14	218.99	-6.77	0.81	-34.69	468.3	247.3
15	224.80	-5.12	1.33	-25.57	837.8	311.9
16	228.17	-6.58	0.45	-10.08	307	18.79
17	228.81	-5.32	0.62	-10.49	423.6	38.27

The 35th bus has more voltage error of 7.8%, which is because of the large power drawn by the nearest voltage regulating transformer. However, bus 49 has more load; therefore, it draws more current than all other buses in SN2.

Table 5. Phase R: Balanced loads simulation results of 207(L-L) voltage buses

Bus no.	V_R volts (rms)	Angle (deg.)	I_R amps (rms)	Angle (deg.)	P_{RYB} watts	Q_{RYB} var
18	118.36	-4.44	0.94	-24.93	313.4	116.8
19	113.58	-7.45	0.24	-32.77	72.41	34.23
20	110.97	-8.62	0.17	-44.77	44.94	32.83
23	116.14	-8.55	0.40	-39.35	118.3	70.4
25	113.63	-9.50	0.36	-32.63	113.2	48.05
27	114.38	-6.96	0.77	-33.09	237.4	116.2
28	116.74	-5.60	0.90	-32.79	278.5	142.7
29	118.45	-4.67	1.67	-25.09	555.6	206.3
30	112.54	-10.31	0.20	-31.37	61.57	23.56
31	111.10	-11.40	0.11	-34.91	33.08	14.34
32	111.83	-10.81	0.04	171.77	-11.74	0.5894
33	111.71	-10.88	0.10	-37.58	29.56	14.81
35	110.16	-10.27	0.54	-42.37	149.5	93.52
38	116.90	-8.21	0.51	6.30	170.3	-44.16
41	116.81	-6.40	0.28	164.10	-97.71	-16.33
42	114.83	-8.63	0.12	-161.24	-37.88	19.55
43	116.47	-6.40	0.05	-7.57	15.68	0.2914
44	116.90	-7.49	0.79	-1.78	273.9	-27.36
47	119.21	-7.84	0.96	-41.12	285.6	186.6
49	122.86	-6.91	2.35	-49.42	639.5	583
50	120.76	-7.76	0.44	-42.83	131.1	91.43
51	121.30	-6.92	0.17	171.00	-61.32	-2.165
52	116.79	-6.10	0.37	-21.27	124.5	33.58
53	116.30	-6.63	0.24	-17.18	82.44	15.25
54	119.18	-5.55	0.32	136.00	-88.28	-69.66
55	122.61	-4.08	0.41	141.98	-126.4	-84.62
56	115.24	-9.67	0.07	107.66	-11.04	-21.02
57	114.33	-9.76	0.13	0.11	43.71	-7.66

Table 6 shows the transformers power flow, these results are useful for finding the rating of transformers while designing the LVSM. More power flew through the distribution transformer connected between 13-49 buses. Grey colored cells in the table show voltage regulating transformers, among those, the transformer connected between 24-25 buses draws more power. However, transformers have almost negligible power losses.

Table 6. Balanced loads- power flow through step-down and voltage regulating transformers

S. no	Fb	Tb	P_{RYB} watts	Q_{RYB} var	S. no	Fb	Tb	P_{RYB} watts	Q_{RYB} var
1	4	18	308.61	128.39	9	9	55	248.67	163.78
2	7	29	567.67	226.41	10	21	20	20.70	5.28
3	11	41	301.47	79.44	11	24	25	151.89	82.48
4	15	45	302.99	45.24	12	24	26	-118.7	-73.81
5	14	46	346.49	271.99	13	34	32	92.99	52.35
6	10	51	293.4	79.46	14	40	56	-39.02	84.23
7	13	49	779.26	687.75	15	39	57	74.53	20.41
8	11	43	18.64	2.10					

Table 7 and Table 8 show power flow in the pi-model transmission lines, some of the lines interconnected between generator buses drawn zero/negligible power and losses shown in grey colored rows. In SN1 among all lines, the line between 12-13 buses has more power flow as well losses.

Table 7. Power flow through π-lines in 414(l-l) voltage section and line power losses

S. no	Line		From bus Power flow		Losses	
	Fb	Tb	P_{RYB} (watts)	Q_{RYB} (var)	P_{RYB} (watts)	Q_{RYB} (var)
1	1	2	0	-2.99	0	0
2	2	3	0	-9.07	0	0
3	3	4	243.85	69.73	0.65	-5.13
4	4	5	-7.2	-22.27	0.01	-17.08
5	4	6	-60.18	-33.22	0.16	-30.8
6	6	7	247.31	94.94	2.05	-13.49
7	6	8	0	-18.49	0	0
8	8	9	0	-5.39	0	0
9	9	10	159	28.42	1.27	-30.21
10	9	11	439.24	228.30	5.87	5.93
11	9	12	0	-31.56	0	0
12	9	13	273.60	168.65	4.79	-13.17
13	13	14	186.21	110.18	0.63	-5.89
14	13	15	-107.99	118.91	0.62	14.72
15	1	15	371.69	197.50	4.57	-0.58
16	1	16	110.32	-20.15	0.69	0.67
17	1	17	237.40	21.50	1.72	-15.95
18	3	15	637.93	349.94	7.85	20.4
19	5	6	-124.21	-30.34	0.28	-12.49
20	7	8	-351.29	-147.16	2.93	-3.19
21	10	12	-209.74	-67.89	1.69	-19.76
22	11	13	83.28	110.84	0.46	-12.67
23	12	13	744.88	498.71	13.04	40.3

S. no	Line		From bus Power flow		Losses	
	Fb	Tb	P_{RYB} (watts)	Q_{RYB} (var)	P_{RYB} (watts)	Q_{RYB} (var)
24	12	16	279.12	-4.05	1.76	2.12
25	12	17	143.35	0.85	1.04	-33.69
26	14	15	-318.84	-266.56	2.87	0.72

Line power flows in SN2 shown in Table 8, more power flew in a line connected between 46-47 buses, but more losses in a line connected between 37-38 buses. Whereas, the effective active and reactive power losses found in LVSM were 93.43watts, 64.75var respectively.

Table 8. Power flow through π-lines in 207(l-l) voltage section and line power losses

S. no	Line		From bus Power flow		Losses	
	Fb	Tb	P_{RYB} (watts)	Q_{RYB} var)	P_{RYB} (watts)	Q_{RYB} (var)
1	18	19	61.44	29.22	0.9	-5.44
2	19	20	30.54	29.26	0.25	-4.45
3	21	22	-50.69	-35.28	0.12	-1.08
4	22	23	148.63	85.61	0.13	0.28
5	23	24	91.50	66.43	0.92	0.32
6	26	27	-147.50	-102.67	2.56	7.12
7	27	28	-234.06	-114.29	1.86	6.21
8	28	29	-276.92	-141.2	1.58	5.5
9	25	30	66.19	24.81	0.3	-1.37
10	30	31	33.89	9.98	0.19	-5.37
11	31	32	-18.29	-10.74	0.08	-8.97
12	32	33	34.01	16.71	0.01	-0.39
13	34	35	-119.60	-78.96	0.5	1.07
14	35	36	-174.10	-107.03	0.68	2.08
15	36	37	-163.32	-220.87	0.83	2.86
16	37	38	-267.00	-272.43	4.31	15.88
17	37	39	102.85	48.69	0.15	0.1
18	36	40	-11.46	111.76	0.17	0.14
19	22	38	-199.44	-119.81	0.44	1.35
20	41	42	112.05	29.09	1.24	9.24
21	41	43	1.23	3.18	0	-5.61
22	38	44	-126.94	43.27	0.28	0.35
23	46	47	283.64	208.65	2.12	7.47
24	47	48	14.52	96.78	0.06	-0.1
25	48	49	-227.87	-202.26	3.12	10.59
26	49	50	87.72	91.41	0.51	0.11
27	50	51	-101.78	-3.193	0.57	-0.983
28	29	52	107.31	25.43	0.62	-0.06

S. no	Line		From bus Power flow		Losses	
	Fb	Tb	P_{RYB} (watts)	Q_{RYB} var)	P_{RYB} (watts)	Q_{RYB} (var)
29	52	53	62.69	5.69	0.11	-0.89
30	53	54	-117.41	-83.41	1.32	2.09
31	54	55	-155.73	-98.10	1.99	4.66
32	44	45	-235.22	26.72	1.9	5.87
33	56	41	-101.50	-1.61	1.58	-1.09
34	56	42	-46.56	16.04	0.25	-3.7
35	57	56	-13.63	-25.78	0.06	-3.19
36	38	49	-229.79	-223.41	4.9	17.08
37	38	48	-240.46	-292.33	1.87	6.81

3.3 Unbalanced loads LVSM

In this test, all constant PQ loads shared as 26%, 34% and 40%, uniformly on R, Y, B phases respectively; therefore, more voltage regulation was found on the B-phase. Table 9 shows, bus 14 has a 9.76% large voltage error and a load angle of 8.35 deg lag in SN1.

Table 9. Voltage magnitude and angle of buses in 414(l-l) VOLTAGE section

Bus no.	V_R volts (rms)	Angle (deg.)	V_Y volts (rms)	Angle (deg.)	V_B volts (rms)	Angle (deg.)
1	234.32	-1.83	233.16	-122.29	231.98	117.41
2	234.34	-1.08	233.42	-121.25	231.89	118.63
3	233.97	-1.92	232.87	-122.35	231.63	117.35
5	235.43	-2.26	233.37	-122.86	232.71	116.83
6	236.09	-1.93	235.40	-122.45	234.58	117.22
8	234.47	-2.64	233.39	-123.35	232.21	116.17
9	232.30	-3.27	230.67	-124.07	229.11	115.34
10	230.11	-5.40	224.20	-126.67	222.89	111.58
12	230.94	-4.98	227.71	-126.40	226.42	112.44
13	225.03	-5.46	218.76	-126.55	217.17	111.63
14	224	-5.47	217.34	-126.47	215.67	111.65
15	228.49	-4.16	223.71	-124.94	222.19	113.76
16	231.99	-4.99	226.31	-126.53		111.80
17	232.64	-4.02	227.04	-125.20	226.77	113.29

Table 10 represents that because of more power drawn by the 34 bus, the preceding 35th has a large voltage error of 10.22%, and the 31 bus has a more voltage angle of 14.42 deg., in SN2.

Table 10. Voltage magnitude and angle of buses in 207(l-l) VOLTAGE section

Bus no.	V_R volts (rms)	Angle (deg.)	V_Y volts (rms)	Angle (deg.)	V_B volts (rms)	Angle (deg.)
18	119.61	-3.55	118.10	-124.43	117.37	114.69
19	116.47	-6.00	112.57	-127.09	111.74	110.78
20	114.35	-7.04	109.84	-128.14	108.78	109.34
23	119.81	-6.93	114.86	-128.05	113.81	109.33
25	117.53	-7.85	112.37	-128.91	111.07	108.27
27	117.12	-5.57	113.35	-126.61	112.72	111.32
28	118.83	-4.47	115.99	-125.38	115.41	113.06
29	120	-3.37	117.93	-124.55	117.42	114.28
30	117.09	-8.49	111.02	-129.57	109.59	107.11
31	116.46	-9.37	109.31	-130.48	107.68	105.58
32	116.50	-8.95	110.34	-130.05	108.74	106.54
33	116.44	-9	110.20	-130.11	108.60	106.44
35	114.52	-8.46	108.73	-129.57	107.30	107.19
37	116.43	-7.79	111.10	-128.90	109.82	108.17
38	120.45	-6.63	115.67	-127.73	114.65	109.75
41	119.07	-5.21	116.18	-126.18	115.18	112.22
42	118.69	-7.04	113.60	-128.07	112.26	109.22
43	118.73	-5.21	115.84	-126.18	114.85	112.22
44	120.10	-6.03	115.76	-127.09	114.87	110.65
47	122.69	-6.28	117.96	-127.40	117.04	110.17
49	125.51	-5.55	121.99	-126.66	121.09	111.51
50	124.15	-6.13	119.52	-127.37	118.65	110.24
51	123.67	-5.47	120.48	-126.76	119.76	111.48
52	119.70	-4.76	115.69	-125.72	115.02	112.18
53	119.69	-5.14	115.01	-126.15	114.27	111.42
54	121.51	-4.38	118.41	-125.31	117.63	113.05
55	123.47	-3.33	122.59	-124.14	121.74	115.26
56	119.40	-7.95	113.88	-129.05	112.50	107.98
57	118.48	-8.02	112.96	-129.14	111.62	107.86

The highest load at bus 12 on phase 'B'; as shown in Table 11, draws the highest current of 5.75 amps. However, the highest angle is 38.84 deg which is at bus 2, in SN1.

Table 11. Current magnitude and angle of buses in 414(l-l) VOLTAGE section

Bus no.	I_R amp (rms)	Angle (deg.)	I_Y amp (rms)	Angle (deg.)	I_B amp (rms)	Angle (deg.)
1	1.54	-24.65	1.93	-144.82	2.21	93.35
2	1.12	-38.84	1.32	-159.88	1.58	75.78
3	1.63	-25.35	1.99	-145.45	2.28	92.64
5	0.04	117.87	0.05	-3.90	0.05	-131.5
6	1.48	-12.95	1.87	-132.76	2.13	105.58
8	2.05	-15.86	2.59	-136.13	2.97	102.86
9	2.61	-20.01	3.23	-140.52	3.72	98.29
10	0.12	-46	0.15	-173.39	0.17	68.74
12	3.80	-15.93	4.92	-138.51	5.75	102.07
13	0.13	97.59	0.16	-28.47	0.16	-150.3
14	0.72	-35.89	0.81	-153.28	0.90	84.59
15	1.16	-25.86	1.33	-144.13	1.49	92.96
16	0.38	-10.83	0.46	-127.69	0.52	107.87
17	0.51	-10.06	0.63	-128.76	0.72	107.25

In SN2, the transformer at bus 13 is heavily loaded so as shown in Table 12 secondary side bus 49 draws the highest current of 2.62 amps on the 'B' phase.

Table 12. Current magnitude and angle of buses in 207(l-l) VOLTAGE section

Bus no.	I_R amp (rms)	Angle (deg.)	I_Y amp (rms)	Angle (deg.)	I_B amp (rms)	Angle (deg.)
18	0.76	-24.01	0.96	-144.81	1.11	93.97
19	0.21	-32.39	0.24	-152.23	0.26	85.91
20	0.16	-44.22	0.17	-164.06	0.18	73.97
23	0.36	-38.83	0.40	-158.98	0.43	79.43
25	0.29	-29.64	0.37	-151.85	0.42	84.11
27	0.68	-33.01	0.77	-152.21	0.85	85.58
28	0.78	-32.53	0.90	-151.98	1	85.89
29	1.39	-24.09	1.69	-144.39	1.93	93.19
30	0.16	-32.35	0.2	-150.32	0.23	84.91
31	0.09	-32.35	0.11	-153.62	0.13	81.63
32	0.03	-173.70	0.04	51.13	0.04	-77.46
33	0.08	-35.56	0.10	-156.67	0.12	79.87
35	0.48	-41.18	0.54	-161.53	0.59	75.67
38	0.45	13.11	0.52	-111.88	0.55	118.93
41	0.24	170.05	0.29	44.84	0.33	-81.27
42	0.12	-156.17	0.13	79.51	0.13	-46.94
43	0.04	1.86	0.05	-127.82	0.05	106.17
44	0.67	3.76	0.8	-120.42	0.9	112.55
47	0.83	-41.99	0.96	-160.45	1.08	78.52
49	2.07	-50.37	2.37	-169.29	2.62	70.81

Bus no.	I_R amp (rms)	Angle (deg.)	I_Y amp (rms)	Angle (deg.)	I_B amp (rms)	Angle (deg.)
50	0.37	-44.56	0.44	-162.04	0.51	77.22
51	0.14	-175.31	0.17	49.93	0.20	-77.69
52	0.29	-16.61	0.38	-140.35	0.44	94.41
53	0.19	-10.84	0.25	-136	0.29	97.18
54	0.27	135.39	0.32	15.83	0.36	-103.8
55	0.34	141.76	0.42	21.89	0.48	-98.27
56	0.07	107.36	0.07	-12.57	0.07	-131.9
57	0.11	10.22	0.13	-119.38	0.15	112.27

Out of all generator buses in SN1, 9 and 12 have high loads; therefore, as shown in Table 13 these two buses draw more power than all other buses. Although, some of the buses are caused by low reverse power flow.

Table 13. Active and reactive powers of buses in 414(l-l) VOLTAGE section

Bus no.	P_{RYB} watts	Q_{RYB} var	Bus no.	P_{RYB} watts	Q_{RYB} var
1	1356	507.4	10	74.81	60.91
2	811.3	561	11	-127.7	-104
3	1391	540.5	12	3583	667.2
4	264.4	7.297	13	-9.91	-90.32
5	-14.92	-23.78	14	501.5	246.6
6	1406	264.2	15	907	312.3
7	363.4	130	16	339.5	27.79
8	1917	421.2	17	469.8	47.6
9	2328	640.3			

In SN2, Table 14 shows buses 29 and 49 found to be heavily loaded; also, some buses have reverse power flow.

Table 14. Active and reactive powers of buses in 207(l-l) VOLTAGE section

Bus no.	P_{RYB} watts	Q_{RYB} var	Bus no.	P_{RYB} watts	Q_{RYB} var
18	346.7	114.6	38	188.2	-47.36
19	76.97	33.3	39	99.95	43.7
20	46.58	31.79	40	-5.922	107.8
21	-26.91	-31.44	41	-107.1	-12.77
22	-27.01	-30.21	42	-41.02	19.7
23	123.6	68.09	43	17.68	-0.241
24	64.17	52.42	44	302.8	-29.82
25	123.5	42.6	45	306.6	-20.67
26	163.1	98.7	46	310	189.4
27	252.6	113.4	47	306.3	181.6
28	299.7	138.8	48	14.56	84.87
29	611.3	200.9	49	681.5	565
30	67.17	20.5	50	143.3	88.74
31	35.55	12.69	51	-68.74	2.257
32	-13.12	1.387	52	140	29.47
33	32.1	13.26	53	93.05	12.15
34	106.1	66.91	54	-96.07	-67.27
35	156.2	88.16	55	139.2	-81.87
36	-157.1	-89.72	56	-10.54	-21.11
37	252.5	244	57	49.71	-8.891

3.4 Results Comparison with Methodology

This section shows the reliability scale of the proposed method; from Figure 2, Figure 3, Figure 4 and Figure 5 are boundary bus parameters of load buses on the 'R' phase. As shown in Figure 2, voltage curves were almost identical but the magnitude variations due to the line voltage drop, all the voltages compared against the nominal voltage (pink) of the bus. As shown in Figure 3, the current at the buses is more than calculated because the methodology considers only connected load current but not lines.

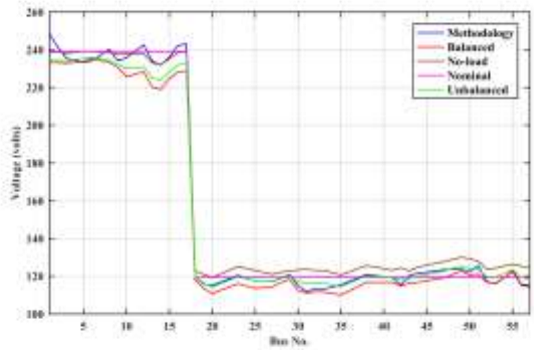

Fig. 2: The voltage at load buses, for all tests with the methodology

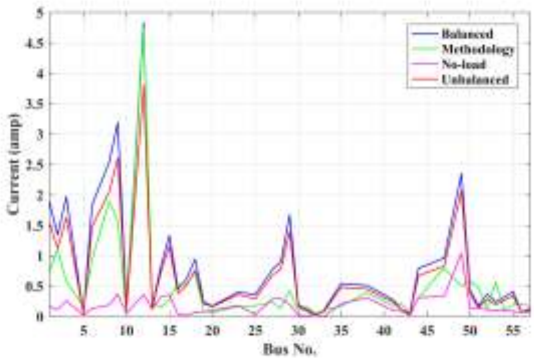

Fig. 3: The current at-load buses, for all tests with the methodology

As shown in Figure 4, between 1 to 10 buses calculated powers show more difference with simulation results.

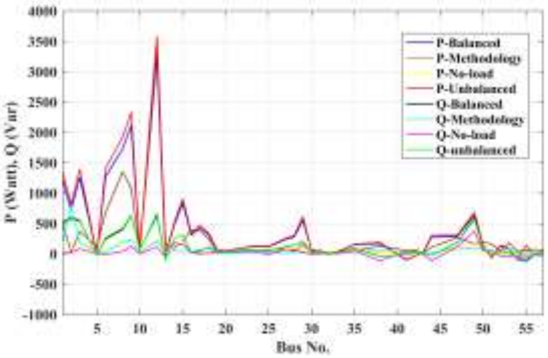

Fig. 4: The power flow at the buses, for all tests and methodology

Figure 5 shows, that bus 2 has very low p.f and some buses show leading p.f because of reverse power flow.

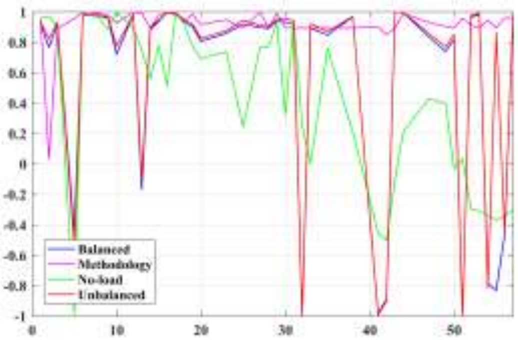

Fig. 5: The p.f at the buses, for all tests and methodology

4 Conclusions

The present paper discussed the development of methodology and procedure to design a 3-phase LVSM of IEEE 57 bus power system in the Simulink platform. Three simulation tests were performed on LVSM to determine the maximum voltage regulation, bus powers, and angles, as well as power, flows in lines, and transformers. Table 15 shows the summary of simulations of SN1 and SN2.

Table 15. Subnetwork wise bus parameters summary

Parameter	No-load		Balanced load		Unbalanced load	
	SN1	SN2	SN1	SN2	SN1	SN2
$\%V_{rmax}$	2.86	1.15	8.37	7.82	9.76	10.22
I_{max} (amp)	0.37	1.04	4.83	2.35	5.75	2.62
δ_{max} (deg.)	-1.12	-2.42	-6.8	-11.4	8.42	14.42
P_{tot} (Watts)	1513.6	1000.8	13620.2	3339.8	15560.1	4997.1
Q_{tot} (Var)	619.6	1089.6	4142.2	1571	4216.1	2224.8
p.f	0.925	0.676	0.956	0.904	0.965	0.913

The main advantage of this work is that the methodology used in this paper is applicable to any standard power system model. However, the LVSM design procedure, and the boundary bus parameters from the results useful for implementing the practical model in the laboratory. While designing, powers are useful to design the rating of equipment, power flows are useful to design pi-lines, voltages to design equipment, and the size of the component by currents. Also, the model can be simulated with real-time simulators either with the required sub-network or the total network.

References:

[1] Issacs, A. (2017). Simulation technology: the evolution of power system modeling. *IEEE Power and Energy Magz*., 15(4), 88-102.

[2] Hay, S., & Ferguson, A. A Review of Power System Modelling Platforms and Capabilities, IET Special Interest Publication for the Council for Science and Technology on "*Modelling Requirements of the GB Power System Resilience during the transition to Low Carbon Energy", IET, London*, 2015.

[3] Katuri, R., & Gorantla, S. (2020). Modeling and analysis of hybrid controller by combining MFB with FLC implemented to ultracapacitor-based electric vehicle. *WSEAS Transactions on Power Systems*, 15, 21-29, https://doi.org/10.37394/232016.2020.15.3.

[4] Teh, J., & Lai, C. M. (2019). Reliability impacts of the dynamic thermal rating system on smart grids considering wireless communications. *IEEE Access*, 7, 41625-41635.

[5] Cheng, Q., Lin, X., Peng, S., Tang, J., Ponci, F., & Monti, A. (2022). Efficient and Robust Power Flow Algorithm for Asynchronous

Grids Coupled Through a VSC-MTDC System and Its Probability Analysis. *IEEE Systems Journ*al, 17(2), 3270-3281.

[6] Zimmerman, R. D., Murillo-Sánchez, C. E., & Thomas, R. J. (2010). MATPOWER: Steady-state operations, planning, and analysis tools for power systems research and education. *IEEE Transactions on power systems,* 26(1), 12-19.

[7] King, J. E., Jupe, S. C., & Taylor, P. C. (2014). Network state-based algorithm selection for power flow management using machine learning. *IEEE Transactions on Power Systems*, 30(5), 2657-2664.

[8] Cole, S., & Belmans, R. (2010). Matdyn, a new matlab-based toolbox for power system dynamic simulation. *IEEE Transactions on Power systems*, 26(3), 1129-1136.

[9] Reddy, C. R., Reddy, K. H., Goud, B. S., & Pakkiraiah, B. (2021). A Deep learning approach for Islanding Detection of Integrated DG with CWT and CNN. *In 2021 International Conference on Sustainable Energy and Future Electric Transportation (SEFET).* pp. 1-7. IEEE.

[10] Triwijaya, S., Sugiantoro, N., Prasetyo, Y., Wibowo, R. S., & Penangsang, O. (2018). Security constrained optimal power flow considering dynamic line rating. *In 2018 10th International Conference on Information Technology and Electrical Engineering (ICITEE), pp.46-51.* IEEE.

[11] Luigi Vanfretti, and Federico Milano, (2012) "Facilitating Constructive Alignment in Power Systems Engineering Education Using Free and Open-Source Software," *IEEE Transactions on Education*, vol. 55, no. 3, pp. 309-318.

[12] Yao, M., Molzahn, D. K., & Mathieu, J. L. (2019). An optimal power-flow approach to improve power system voltage stability using demand response. *IEEE Transactions on Control of Network Systems*, 6(3), 1015-1025.

[13] Martins, R., Kreimer, P., & Musilek, P. (2017). Avelino J. Gonzalez, Robert A. Morris, Frederic D. McKenzie, Daniel J. Carreira, and Brian K. Gann, "Model-Based, Real-Time Control of Electrical Power Systems," *IEEE Transactions on Systems, Man, and Cybernitics-Part A: Systems and Humans*, vol. 26, no. 4, pp 470-482, July. 1996.

[14] Li, S., Wang, D., Zhu, Y., Liu, L., & Jia, H. (2020). Multi-objective optimal control based on practical security region of regional integrated energy system. *In 2020 IEEE Power & Energy Society General Meeting (PESGM)*, pp. 1-5. IEEE.

[15] Chen, P., Sun, K., Zhang, C., & Sun, B. (2021). A Feasible Zone Analysis Method with Global Partial Load Scanning for Solving Power Flow Coupling Models of CCHP Systems. *Journal of Modern Power Systems and Clean Energy*, 10(2), 371-377.

[16] Campanhol, L. B. G., Da Silva, S. A. O., De Oliveira, A. A., & Bacon, V. D. (2018). Power flow and stability analyses of a multifunctional distributed generation system integrating a photovoltaic system with a unified power quality conditioner. *IEEE Transactions on Power Electronics*, 34(7), 6241-6256.

[17] Srikanth, M., Pakkiraiah, B., Upadhyay, P., & Kalyani, S. T. (2019). Dual-mode photovoltaic bidirectional inverter operation for seamless power transfer to dc and AC loads with the grid interface. *International Journal of Photoenergy*, 2019, 1-14.

[18] Goyal, S., Ledwich, G., & Ghosh, A. (2010). Power network in loop: A paradigm for real-time simulation and hardware testing. *IEEE Transactions on Power Delivery*, 25(2), 1083-1092.

[19] Mengshoel, O. J., Chavira, M., Cascio, K., Poll, S., Darwiche, A., & Uckun, S. (2010). Probabilistic model-based diagnosis: An electrical power system case study. *IEEE Transactions on Systems, Man, and Cybernetics-Part A: Systems and Humans*, 40(5), 874-885.

[20] Wijeweera, G., Annakkage, U. D., Zhang, W., Rajapakse, A. D., & Rheault, M. (2017). Development of an equivalent circuit of a large power system for real-time security assessment. *IEEE Transactions on Power Systems*, 33(4), 3490-3499.

[21] Katuri, R., & Gorantla, S. (2020). Realization of prototype hardware model with a novel control technique used in electric vehicle application. *Electrical Engineering*, 102(4), 2539-2551.

[22] Magrini, Ray D Zimmerman and Carlos E Murillo-S´anchez. Matpower 6.0 user's manual. *Power Systems Engineering Research Center*, 2016.

[23] Henriques, R. M., Passos Filho, J. A., & Taranto, G. N. (2021). Determining Voltage Control Areas in Large Scale Power Systems Based on Eigenanalysis of the QV Sensitivity

Matrix. *IEEE Latin America Transactions*, 19(02), 182-190.

Contribution of Individual Authors to the Creation of a Scientific Article (Ghostwriting Policy)

The authors equally contributed to the present research, at all stages from the formulation of the problem to the final findings and solution.

Sources of Funding for Research Presented in a Scientific Article or Scientific Article Itself

We would like to show our gratitude to Vignan's Foundation for Science, Technology, and Research for their encouragement during this work.

Conflict of Interest

The authors have no conflicts of interest to declare.